Indian Journal of Natural Products and Resources
Vol. 15(3), September 2024, pp. 402-412
DOI: 10.56042/ijnpr.v15i3.7842

Fungal Mannosyltransferase as a target to control *Magnaporthe oryzae* through natural bioactive compounds – A bioinformatics approach

Pravallika Darru, Raghavendra Rao Sambangi and Uday Bhaskar Sajja*

Department of Biotechnology, Dr. B R Ambedkar University, Srikakulam, Etcherla, Andhra Pradesh 532410, India

Received 06 January 2024; revised received 13 March 2024; accepted 19 April 2024

Magnaporthe oryzae is a filamentous ascomycete fungus and causes a polycyclic disease called rice blast, which causes the farmers approximately 10 to 30% yield loss. Along with chitin, Glycans are important components of a fungal cell wall, and disruption of them results in compromising the fungal cell integrity. The inhibition of mannosyltransferase is one of the key enzymes involved in the biosynthesis of glycans, which compromises cell wall development and prevents the spread of the disease. The homology-modelled structure of mannosyltransferase was docked against nine natural bioactive compounds from *Annona Squamosa*, *Azadirachta Indica* and *Curcuma longa*, from among which Anonaine from *A. squamosa* recorded the highest docking score of -8.2. This complex was subjected to *in-silico* molecular dynamic simulation (MDS) using GROMACS. During molecular dynamic simulations, post 60 ns, the RMSD value was observed to settle down to 0.8 nm. The plot suggests that the protein acquired stable confirmation post 60 ns without much fluctuation. The majority of the residues of mannosyltransferase showed RMSF less than 0.3 nm. 2 peaks were observed in 100 ns simulation, from 200 to 230 residues and 280 to 300 residues where the RMSF value is greater than 0.3 nm, which indicates that these regions are flexible. The MDS results show that the complex is stable and can form under natural conditions. Our *in silico* docking studies and MDS revealed anonaine from *A. squamosa* as one of the natural compounds capable of binding to mannosyltransferase, which thereby may compromise the assembly of one of the major components of the fungal cell wall, i.e. Glucans.

Keywords: *Anonaine*, Homology modelling, *Magnaporthe oryzae*, Mannosyltransferase, Molecular docking, Molecular dynamic simulations

IPC code; Int. cl. (2021.01)−A01N 65/00, A01P 3/00

Introduction

Rice is the staple food for more than 3 billion people worldwide. Major paddy-producing countries in the world are India, Bangladesh, China, Thailand, Philippines, Myanmar, and Japan. Paddy cultivation is the majority farming activity and source of income for millions of households in these countries. Around 30% of the annual paddy harvest is lost due to biotic and abiotic factors. Among the biotic factors, Fungi are the major contributors to the yield loss. During heavy infestation, rice blast fungus *Magnaporthe oryzae* may singly cause between 10 to 30% loss of the annual rice harvest[1]. Rice blasts caused by the fungus *M. oryzae* are significant economic and humanitarian problems. It is estimated that each year, enough rice is lost due to rice blast disease to feed 60 million people (Fig. 1)[2].

The paddy growing area of Andhra Pradesh and Orissa has stagnated to around 4.5 million hectares, around 10% of the country's total rice cultivated area[3]. Improving productivity by using best agronomic practices, stress management, and Nutrient management plays a significant role in achieving yield improvement[4].

Physiology of *Magnaporthe oryzae*

Depending on the variety and environmental conditions, the pathogen *M. oryzae* produces lesions over leaves (leaf blast), leaf collars (collar blast), culms, culm nodes, panicle neck nodes (neck rot), and panicles (panicle blast), which vary in colour and shape[5]. *M. oryzae* is a filamentous ascomycete fungus, and rice blast is a polycyclic disease spread by asexual spores (conidia) that infect above-ground tissues of rice plants[6]. The fungus infects the rice plant through an infection cell called appressorium. This spore apex contains an adhesive with which the fungus sticks firmly to the tough cuticle of the rice plant. During this attachment, a pressure-driven mechanism breaks the tough cuticle. This mechanism generates a turgor pressure of up to 8.0 MPa that ruptures the cuticle of the affected rice plant[7]. The

*Correspondent author
Email: udaybsajja@gmail.com

Fig. 1 — a) Field showing damage with Rice blast; and b) Close-up of paddy leaves affected with Blast fungus at Addapuseela, parvathipuram Mandal.

appressorium produces a specialised hypha, a penetration peg, which pierces the plant's leaves surface[8]. Upon reaching the epidermal cell lumen, the penetration peg of conidia expands to form a tiny, narrow filamentous primary hypha. The peg then becomes a conduit for moving the nucleus and cytoplasmic contents of the host from the appressorium into the growing primary hypha. This primary hypha becomes a thick, bulbous invasive hypha, which then moves to the neighbouring cells[9]. This will allow the host-pathogen to infect epidermal cells with bulbous invasive hyphae, which proliferate and grow from one cell to another cell[10]. After complete penetration into the host cell, the fungus forms spores through appressorium. Transfer of these spores from one plant to another leads to the spread of the disease in the entire field, which results in a considerable decrease in crop yield.

Disease Management

Agronomic practices such as enriching the soil with high organic matter increase biological activities and are essential for growing healthy paddy. Heavy use of nitrogen fertilisers increases the susceptibility of rice plants to blast[11]. Hence, split application of nitrogen fertilisers is recommended for blast disease management in susceptible cultivars. Cultivars which show a higher accumulation of silicon, which acts as a physical barrier against blast disease, were shown to have less incidence of blast[12].

Mancozeb is a widely used chemical fungicide for the management of blasts. Tricyclazole, in combination with Hexaconazole, has shown the highest disease control, resulting in higher grain yield[13]. Powder formulation of pseudomonas fluorescence at 10 gm/kg is used as a biological control against rice blast[14]. In developing and third-world countries, small farmers who cannot afford chemical fungicides, under integrated management practices, use plant extracts as precautionary measures for repelling pathogens and pest infections. Allicin from garlic and Neem extract were shown to be successful in reducing the fungal spread[15].

Glycosyltransferases

Most of the fungicides used against *M. oryzae* target the enzyme Glycosyltransferase, a key regulatory enzyme in synthesising glycosylated enzymes. In addition to chitin and other proteins, the cell wall is also composed of various sugars, which are important for maintaining the integrity of the cell wall. The cell wall is composed of a number of unique interconnected polysaccharides, including chitin (10 to 20%) and a variety of glucans about (50 to 60%), which the mammalian cells lack. Although rigid, the cell wall is dynamic enough to allow for budding and growth[16]. Glycosyltransferases are ubiquitous and are found in prokaryotes to humans and catalyse the transfer of monosaccharide moieties to biological substrates, including proteins, lipids and carbohydrates[17,18]. The biosynthesis of glycans is primarily determined by the glycosyltransferase that assembles monosaccharide moieties into linear and branched glycans chains. The vast majority of these Glycosyltransferases are responsible for elongating glycan chains[19,20]. It plays an important role in the biogenesis and functions of proteins by influencing their folding, intracellular localisation, stability and solubility. N-glycans are also synthesised by Glycosyltransferase[21].

Bioactive compounds

Anonaine, Asimilobine, Corypalmine, Nornuciferine and Reticuline are bioactive benzyl isoquinoline alkaloids, present in members of the plant families *Magnoliaceae* and *Annonaceae*. They are named after the plant they were first extracted from *Annona reticulate*, which is commonly known as *Annona*[22]. Azadirachtin, Nimbin and Nimbolin -B are extracts of fruit and plant parts of Neem. These compounds are shown to regulate the metamorphosis process of insects that are passing from the larval stage to the pupal stage[23]. Curcumin is a bioactive compound extracted from Curcuma longa of the Zingiberaceae family and sold as a herbal supplement, cosmetic ingredient, food flavouring and colouring agent[24].

Though many studies have established the effectiveness of natural concoctions against certain pests and fungi crudely, a Bioinformatics approach is made in this present study to identify plant-based bioactive compounds against one of the key enzymes involved in the cell wall synthesis pathway is mannosyltransferase. A protein-ligand docking study, in this case, mannosyltransferase and nine bioactive compounds from neem, custard apple, and turmeric, will establish a specific bioactive compound which can be used against major plant disease-causing fungi.

Material and Methods

Homology modelling

Homology modelling is one of the computational structure prediction methods that use segments of amino acid sequences to compare with existing confirmed protein 3D structures to predict the structure of a given amino acid sequence. It is considered to be the most accurate of the computational structure prediction methods. Since the functionality of the model depends on the quality of the generated protein 3D structure, maximising the quality of homology modelling is crucial. Generally, the process of homology modelling involves four steps: target identification, sequence alignment, model building and model refinement. The sequence of mannosyltransferase was taken from UniProtKB (ID – G4MPW0_PYRO7) and given as input to a web-based suite with advanced remote homology modelling methods to build 3D models. The 3D structure was modelled using SWISS-MODEL[25], which gave 20 models in which we took the highest reliability with 100% sequence similarity of *M. oryzae*. After building the model, the structure was downloaded from the server and visualised using PyMOL. Procheck analysis was carried out in saves.mbi, a web-based server to confirm the 3-D structure of the modelled mannosyltransferase, and Errata was used to verify its quality factors and sequence alignment[26].

Ligand preparation

Many natural concoctions are used by farmers from South India in which leaves of various plants are used as one of the compositions. The most commonly used plant parts are from Neem, Custard Apple, and rhizomes of turmeric. The leaves of neem contain bio compounds Azadirachtin (AZR), Nimbin (NM) and Nimbolin-b (NM-b). Anonaine (AN), Nornuciferine (NNF), Corypalmine (CP), Asimilobine (ASL) and Reticuline (RTL) are bio compounds commonly found in Custard Apple, whereas Curcumin (CM) is found in Turmeric rhizomes. The nine naturally occurring compounds widely used in natural concoctions were selected to check their binding capacity of mannosyltransferase in fungi using an *in-silico* molecular docking strategy. All the 3-D structures of the nine natural compounds were downloaded from the PubChem database and saved in PDB format (Fig. 2). The molecular docking was performed by using the selected nine natural compounds against homology-modelled mannosyltransferase.

Identification of the active site of mannosyltransferase

The generated 3-D structure of mannosyltransferase in PDB format was submitted to the CastP 3.0 server, and the active site residues and binding pockets were recovered, which were used to specify grid box coordinates (Fig. 3)[27]. The active site residues are 65 TRP, 66 ASP, 70 PHE, 78 TYR, 84 TRP, 85 ALA, 86 PHE, 87 GLU, 88 GLU, 163 PHE, 168 TYR, 216 THR, 217 THR, 218 PHE, 219 ARG, 220 THR, 221 ASN, 266 SER, 269 PRO, 270 GLN, 300 TYR, 304 GLN, 308 TRP, and 383 TYR.

Molecular docking

Molecular docking was performed using PYRX to screen the nine compounds against mannosyltransferase. PYRX works on empirical–based free energy scoring and Lamarckian genetic algorithm using Autodock Vina[28]. All the ligands and macromolecules are converted from PDB to PDBQT format by choosing the auto dock option in PYRX. Molecular docking was performed in the grid box generated on the X, Y, and Z axes. Dimensions were adjusted as grid centre X: 57.0712, Y:-15.395 and Z: 26.4746 with a spacing of 1.5450 A° based on the binding site information given by the castp3.0, with exhaustiveness of 8 for docking, and the calculations were conducted in such a manner that only lowest energy poses was obtained as an output. The Docking results were analysed based on binding energy scores. All ligands displayed acceptable binding energy scores. All the nine ligands in PDBQT format were docked with homology-modelled manno-syltransferase.

Molecular dynamic simulations

To evaluate the conformational changes in the protein structure induced by the ligand, the complex was subjected to Molecular Dynamic simulation lasting 100 ns. The implementation of the CHARMM36 force field in the GROMACS 2021.2 software package was utilised for conducting MD simulations (https://ft.gromacs.org/gromacs/gromacs-2021)[29]. The Cgenff server was

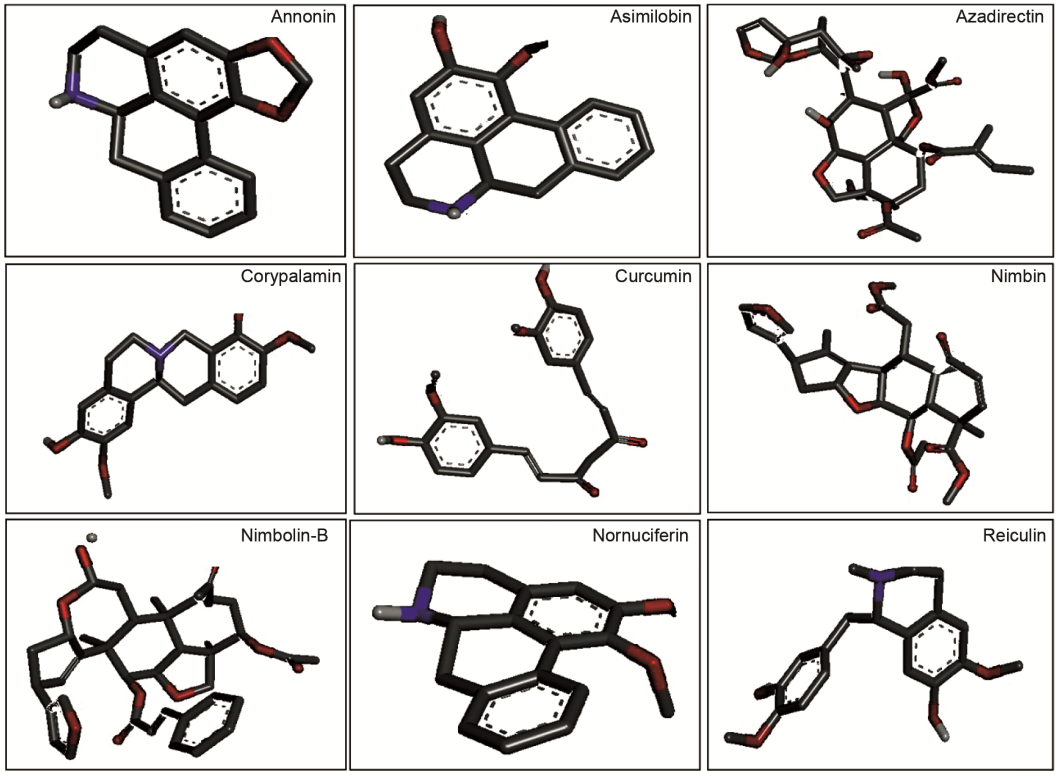

Fig. 2 — Structures of bioactive compounds downloaded from PubChem dataset AZR, NM, NM-b is from *Azadirachta indica.* AN, NNF, CP, ASL, and RTL are bioactive compounds found in *Annona squamosa.* CM is from *Curcuma longa* rhizomes.

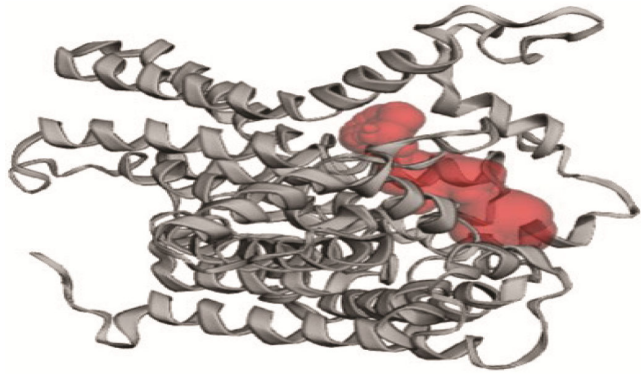

Fig. 3 — Homology-modelled mannosyltransferase showing active sites and binding pockets as predicted by the castp3.0 online tool.

employed to produce the topologies and parameter files for the lead compound[30]. The solvation of the ligand-protein combination was performed using the transferable intermolecular potential with a three-point (TIP3P) water model. The complex was recreated using a dodecahedron-shaped box with a buffer distance of 1 Å. The neutrality of the system was achieved through the incorporation of Na+ and Cl- ions into the system. By employing the technique of energy reduction and doing 5,000 iterations of the steepest descent method, the presence of unfavourable connections and collisions within the protein structure were successfully mitigated. The entire system was subjected to heating at a temperature of 310 K. During the 100 ns production run, a system that had reached equilibrium was employed at constant temperature and pressure. Post-MD analysis included RMSD, RMSF, SASA, Rg and hydrogen bonds.

Results and Discussion

Homology modelling

This study provides comprehensive details on targeting fungal cell wall component mannosyl transferase using homology modelling, molecular docking-based virtual screening and free energy calculations. Homology modelled structure of mannosyltransferase was created and downloaded from the Expasy tool SWISS-MODEL (Fig. 3). Alpha Fold DB model of L7JF69_MAGOP showed the highest similarity with gene L7JF69_MAGOP, organism: *Magnaporthe oryzae* (strain P131) Rice blast fungus.

Mannosyltransferase of *M. oryzae* amino acid sequence was taken from the UniProt database (G4MPW0_MAGO7), and a 3D model was constructed using SWISS-MODEL. The model was validated by

Table 1 — Distribution of amino acids within the Ramachandran plot

Ramachandran plot Statistics		
Residues in most favoured regions [A,B,L]	356	93.4%
Residues in additional allowed regions [a,b,l,p]	25	6.6%
Residues in generously allowed regions [~a,~b,~l,~p]	0	0.0%
Residues in disallowed regions	0	0.0%
Number of non-glycine and non-proline residues	381	100.0%
Number of end-residues (excl. Gly and Pro)	2	
Number of glycine residues (shown as triangles)	30	
Number of proline residues	26	
Total number of residues	439	

The table shows the percentage of residues in the most favoured region (A, B, L) and additionally allowed regions (a, b, l, and p) and location of glycine, proline residues

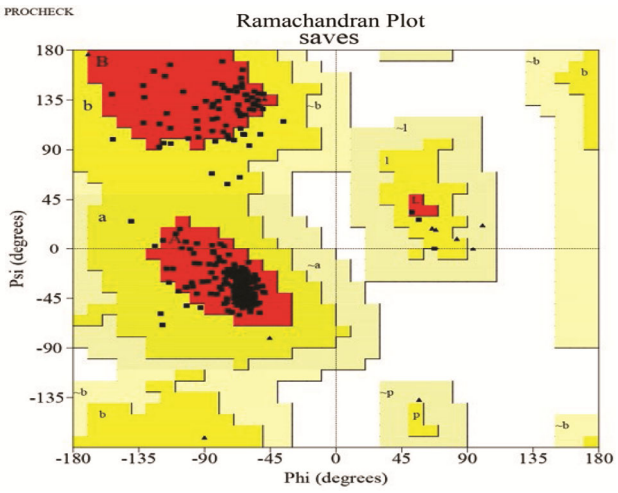

Fig. 4 — Ramachandran plot of homology modelled mannosyltransferase showing residues in most favoured regions (A, B, L) and additionally allowed regions (a, b, l, p).

using the Ramachandran plot. Out of the 381 non-glycine and non-proline residues, 356 are within the most favoured region (A, B, L) (93.4%), and 25 are in the additionally allowed region (a, b, l, p) (6.6%) (Table 1) (Fig. 4). Quality of the protein sequenced was validated by using ERRAT Application which showed 97.862% overall quality factor. Glob plot analysis was done to identify conserved domains, which revealed the presence of Tran's membrane domain in the region from 21-422.

Docking studies of *Annona squamosa* bioactive compounds with Mannosyltransferase

The goal of ligand-protein docking is to predict the predominant binding mode(s) of a ligand with a protein of known three-dimensional structure. The virtual screening software PYRX was used to carry out the molecular docking studies. PYRX tool works on the empirical binding, free energy scoring and Lamarckian genetic algorithm. All the ligands and macromolecules were converted from PDB to PDBqt format by choosing the auto dock option in PYRX. Molecular docking was performed as in the grid box generated in X, Y and Z axis X: 57.0712, Y:-15.395 and Z: 26.4746 based on active site predicted by CastP 3.0. *Annona squamosa,* a common tropical and sub-tropical plant, is known for its bioactive compounds having insecticidal and fungicidal properties[31]. The binding ability of AN, NNF, CP, ASL, and RTL compounds was checked against mannosyltransferase using a molecular docking technique. The enzyme's active site was kept in a grid box for docking with the above bioactive compounds. Mannosyltransferase binding amino acids with bioactive ligands of *A. squamosa* was given in Table 2.

Molecular docking of AN with mannosyltransferase showed ARG186, CYS184, TYR202, HIS54, TRP55, and TYR57 as interacting amino acids with a docking score of -8.2. (Fig. 5) In addition to Anonaine, NNF CP, ASL and RTL were also docked with mannosyltransferase, and their docking score, along with the interacting Amino acids, were detailed in Table 2. Among the natural bioactive compounds of *A. squamosa* tested against mannosyltransferase, Anonaine (AN) showed the highest docking score of -8.2kcal/mol. Studies have shown that (+)-anonaine has strong inhibitory activities against *Bacillus cereus*, *Escherichia coli*, *Micrococcus* sp., *Staphylococcus aureus* and *S. epidermidis* and displays anti-fungus activities against *Trichophyton rubrum* and *Microsporum gypseum* growth[32].

Docking of Neem bioactive compounds and curcumin with mannosyltransferase

Historically, Neem leaves and seed extracts have been used by farmers as repellents to protect crop plants against various pests and pathogens. The three well-documented bioactive compounds from *Azadirachta indica* are AZR, NM and NM-b. The three bioactive compounds from neem were docked with mannosyltransferase by taking the active site of the enzyme in the grid. The binding amino acids and a score of mannosyltransferase with bioactive compounds of neem are shown in Table 2. Among the compounds, NM-b showed the highest binding score with -7.6 kcal/mol when docked with mannosyltransferase, as shown in (Table 2). Curcumin, a powerful

Table 2 — Docking score of 9 bioactive compounds against mannosyltransferase AZR, NM, NM-bare from *Azadirachta indica*, AN, NNF, CP, ASL, and RTL bioactive compounds found in *Annona squamosa*. CM is from *Curcuma longa* rhizomes

S. No	Enzymes/Bio Compound	Interacting amino acids/ Pocket amino acids	Docking Score k.cal/mol
1	Anonaine (AN)	ARG186, CYS184, TYR202, HIS54, TRP55, TYR57	-8.2
2	Asimilobine (ASL)	HIS335, LEU317, TRP324	-7.0
3	Corypalmine (CP)	GLU214, ARG210, ARG211, SER226, CYS227, TYR207, LEU334, ALA337, ASN309, SER341.	-6.6
4	Nornuciferine (NNF)	TRP254, LEU420, TRP310, TRP314, VAL318.	-7.2
5	Reticuline (RTL)	ILE412, TRP300, LEU299, PHE408, TRP200.	-6.9
6	Azadirachtin (AZR)	ILE412, TYR415, LEU299, ARG317	-6.8
7	Nimbin (NM)	ARG307, TYR300, LEU299, ILE412, PHE408	-7.1
8	Nimbolin –B (NM-b)	ILE296, TYR300, LEU299, ILE410, PHE408, TYR415	-7.6
9	Curcumin (CM)	LEU299, TYR300, SER303, ARG307, ILE412, TYR415	-6.2

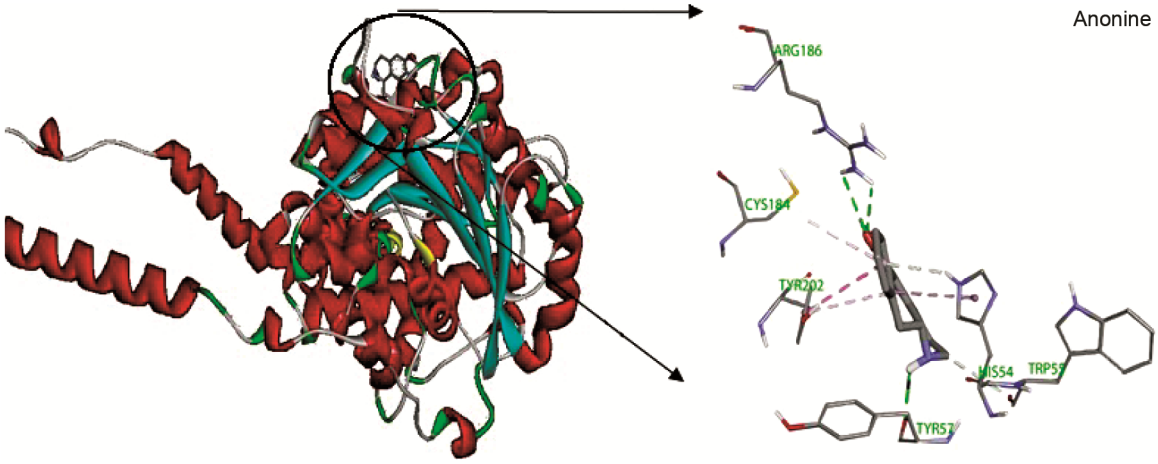

Fig. 5 — Interaction of bioactive compound anonaine from *Annona squamosa* with Mannosyltransferase.

immune modulating compound, is an orange-yellow polyphenolic and hydrophobic phytochemical component of the turmeric herb *Curcuma longa* L. Among its many uses, Curcumin is widely used to prepare natural concoctions against plant diseases. When docked with mannosyltransferase, curcumin exhibited a binding score of -6.2 kcal/mol (Table 2).

Molecular dynamic simulations (MDS), RMSD of enzyme-substrate complex

Molecular dynamic simulations provide greater insight into ligand-protein interactions with regard to conformational stability, flexibility, compactness and surface accessibility. RMSD measures the deviation between the coordinates of atoms of bimolecular structures in a simulated state compared to a reference structure. It is measured by calculating the root mean square of the differences in atomic coordinates of the simulated structure to the reference structure at corresponding atoms. The root mean square value is often used to assess the stability of the interaction during molecular dynamic simulations[33]. The root mean square deviations (RMSD) of protein C alpha atoms were considered the reference for calculating the RMSD. The initial RMSD was at 0.2 nm during molecular dynamic simulations, which increased to 0.6 nm at the first 10 ns. However, the RMSD value gradually increased to 0.8 nm from 10 to 40 ns. Post 60 ns, the RMSD value was observed to settle down to 0.8 nm. The few fluctuations observed initially indicate a conformational change in the protein upon binding to the ligand. The plot suggests that the protein acquired stable confirmation post 60 ns without much fluctuation[34] (Fig. 6a, 6b).

Enzyme substrate complex RMSF

A root mean square fluctuation (RMSF) measures the flexibility of individual atoms or groups of atoms within a protein structure over time during the molecular dynamic simulation. High RMSF values indicate flexibility in the residues, whereas low RMSF

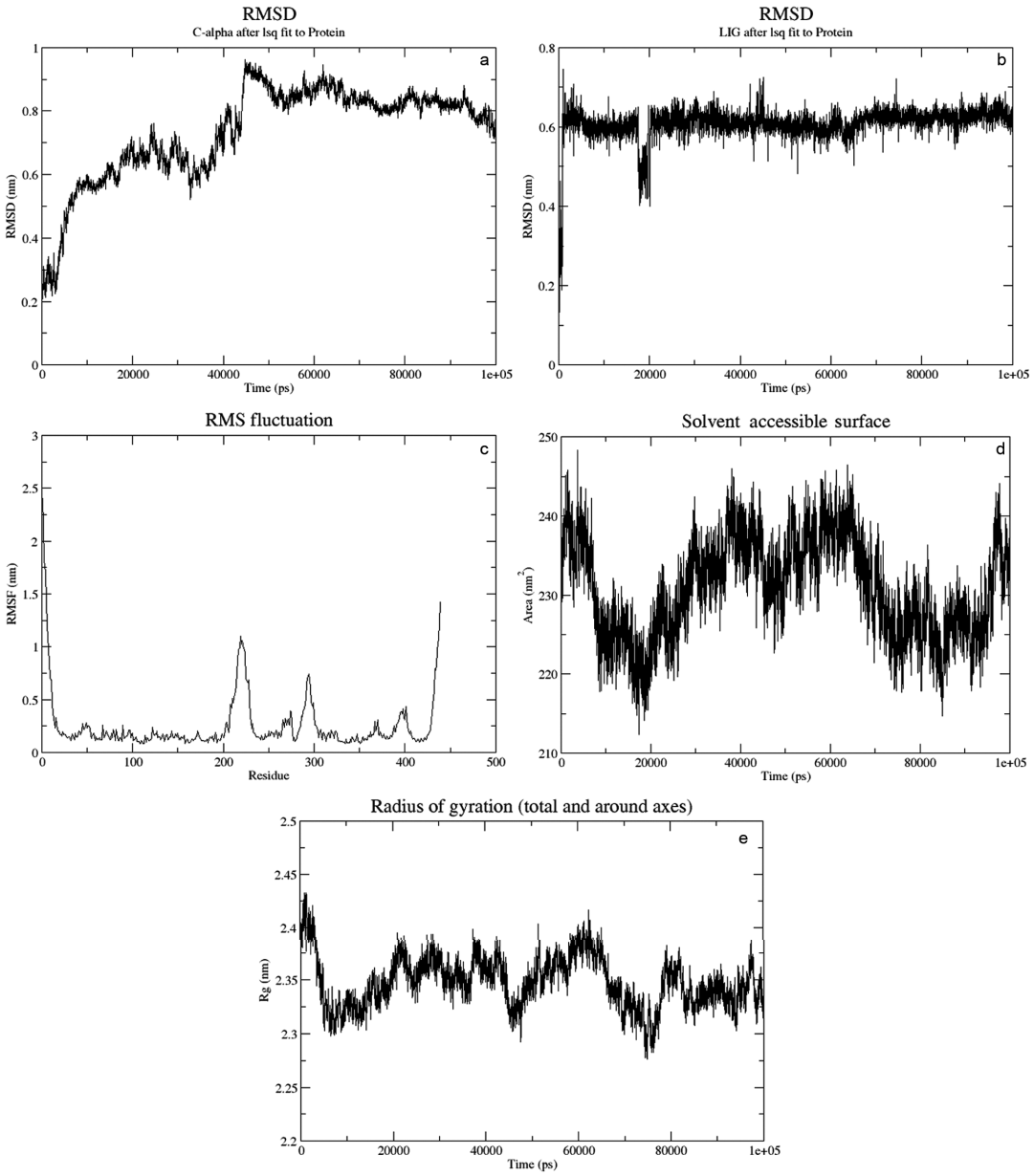

Fig. 6 — Molecular dynamic simulation trajectories. a) RMSD of the protein C-α atoms when bound to the ligand during the 100 ns MD simulation; b) RMSD of the ligand when bound to the protein during the 100 ns MD simulation; c) RMSF of the protein when bound to the ligand during the 100 ns MD simulation; d) SASA of the protein when bound to the ligand during the 100 ns MD simulation; and e) Radius of gyration of the protein when bound to the ligand during the 100 ns MD simulation.

values indicate rigidness in the amino acid residues of the enzyme. RMSF analysis reveals regions in the protein that may be functionally important**.** Molecular dynamic simulations of mannosyltransferase bound with Anonaine are shown in (Fig. 6c). Majority of the residues of mannosyltransferase showed RMSF less than 0.3 nm. 2 peaks were observed in 100 ns simulation, from 200 to 230 residues, and 280 to 300 residues were RMSF value is greater than 0.3 nm. As per our CastP 3.0 analysis, the two peaks observed between 200 to 230 residues and 280 to 300 residues fall under the active sites of mannosyltransferase, which indicates flexibility in the active site region. The flexibility of this region allows the ligand to be stably bound.

Solvent accessible surface area (SASA)

The analysis of Solvent Accessible Surface Area (SASA) for the protein during the 100 ns simulation offers a dynamic perspective on the protein's

interaction with its surrounding solvent environment. Fig. 6c shows the SASA of the protein when bound to the ligand. Initially, the SASA was measured at 240 nm², reflecting the extent of the protein's surface accessible to the solvent. A minor decrease was observed over the first 50 ns, indicating potential adjustments in the protein's surface interactions. However, for most of the 100 ns simulation, the SASA stabilised at approximately 230 nm². This consistent SASA suggests that, after an initial phase of adaptation, the protein maintained a well-defined surface conformation, allowing it to interact consistently with the solvent environment. These findings shed light on the protein's stability and ability to maintain specific interactions throughout the simulation, contributing to our understanding of its structural dynamics and behaviour (Fig. 6d).

The analysis of the radius of gyration

Rg for the protein reveals a remarkable consistency and maintenance of protein globularity throughout the simulation (Fig. 6e), showing the Rg of the protein when the ligand. The Rg values remained within the 2.35 to 2.4 nm range, indicating that the protein's overall compactness and structural integrity were effectively preserved. The steadiness in Rg values indicates the protein's ability to maintain its well-defined and globular conformation, which is crucial for functional stability. This consistency in Rg values underscores the reliability and structural robustness of the protein during the entire simulation, emphasising its capacity to maintain its essential structural characteristics. The examination of protein-ligand interactions, as depicted in (Fig. 7), provides critical insights into the stability of the binding over the course of the 100 ns simulation. Notably, at the beginning of the simulation (0 ns), five pi-alkyl bonds were formed, indicating strong initial interactions between the ligand and the protein. Importantly, most of these bonds remained constant throughout the 100 ns simulation, signifying the preservation of the binding conformation between the ligand and the protein. This consistency suggests that the protein-ligand complex maintained a stable and unaltered binding mode over the entire simulation duration. The robustness of these interactions is a promising sign, highlighting the durability of the ligands' association with the protein and the potential suitability of this binding conformation for further drug development or structural studies[35]. From the predicted RMSD, RMSF and Radius of gyration values, together with the predicted Hydrogen bonding between Anonaine and the target mannosyltransferase, it could be concluded that the bioactive compound – Anonaine present in *A. squamosa* interacts efficiently with Manno-syltransferase.

Discussion

Magnaporthe oryzae, which causes blast disease in rice, is a major challenge in disease management. Though a good number of fungicides are available in the market, the fungus is resilient, and a number of strains are being observed that show a marked resistance to the existing fungicides. Due to this reason,

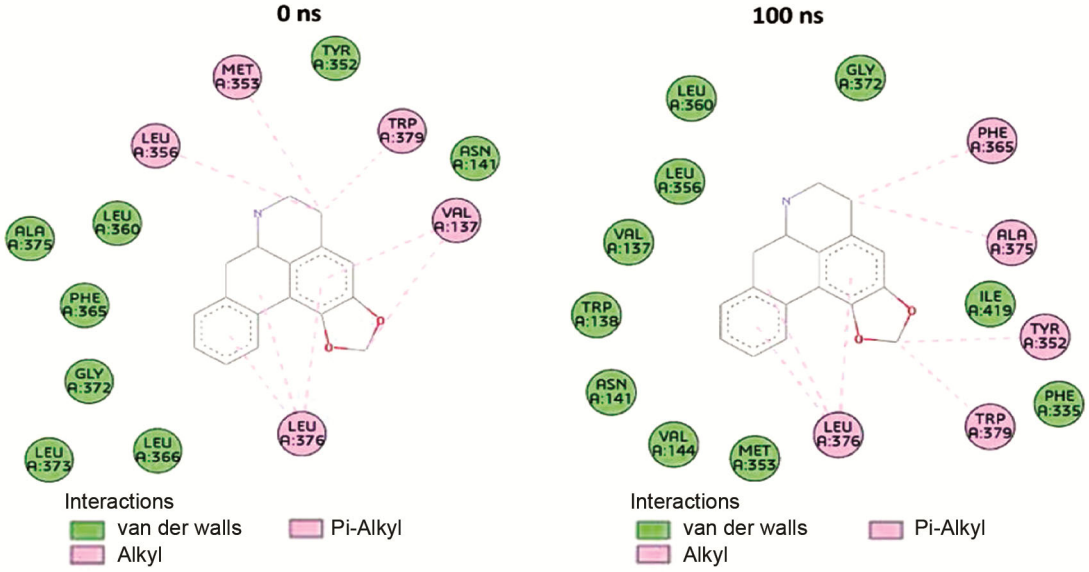

Fig. 7 — Interaction plot between protein and ligand at the initial 0 ns and 100 ns MD simulation.

comprehensive disease management strategies are being suggested to the farmers, which include good agronomic practices, resistant varieties, biological control, and usage of bioactive compounds from natural sources in addition to fungicides for the management of fungal diseases[36]. Bioactive compounds from plant sources are being increasingly used by farmers because of the ease of availability of source materials and ease of preparation as a part of including organic/natural farming components in disease management practices. In preparation for these natural concoctions, farmers typically use locally available plant sources such as neem, custard apple, and turmeric in Indian subcontinent. Comparative transcriptome analysis Studies conducted by Deng *et al.* on type – 2 glycosyltransferases revealed the importance of glycosyltransferases in modifying glycoprotein, which is important in *M. oryzae* infection-related morphogenesis and pathogenesis[37]. Glycosyltransferases are unique enzymes that transfer monosaccharide moieties onto glycans, giving stability and involvement in surface binding. Sahar and Jeffery *et al.* argue the need for alternative antifungal agents given increasing resistance among fungal pathogens[36]. They suggest targeting the pathways synthesising N-linked and O-linked oligosaccharides that reside on the exterior mannoproteins. Mannosyltransferase and glycosyltransferases located in the Golgi complex play an important role in synthesising these oligosaccharides.

In this study, we used a ligand-based molecular docking approach to screen bioactive compounds from *A. squamosa*, *A. indica*, and *C. longa* as ligands and 3D structure of mannosyltransferase as a macro molecule to identify a good bioactive compound against *M. oryzae*. The homology-modelled mannosyltransferase generated was used for molecular docking[38]. The protein-ligand interactions targeted the functional residues that constituted the active sites and were in a good docking pose with the least binding energy. Among the screened compounds, Anonaine, with a docking score of -8.2 kcal/mol with mannosyltransferase, shows that it is a potential compound for blocking the enzyme**.** When we docked the chitin Synthase of *M. oryzae* with the selected nine bioactive compounds *in-silico*, it revealed Anonaine as a potential bioactive compound. A study by Deshmukh *et al.*, with Cold ethyl alcohol extract of *A. squamosa* seeds against insect herbivores, indicated that Annona contains useful bioactive compounds that can be used to control agriculture pests and pathogens[39]. Our *in-silico* study also highlights the availability of useful natural molecules of *A. squamosa*, which can be used as potential broad-spectrum biofungicides.

Conclusion

M. oryzae a prolific disease-causing fungus in paddy crop is resistant to current fungicides. It is also observed that the fungus is quick to mutate and become resistant to chemical fungicides. Given this a comprehensive disease management system need to be adopted to manage the infection that includes good agronomic practices, moderate use of fungicides when necessary, use of bio fungicide like Trichoderma and spraying of natural concoctions containing plant extracts. This study using a bioinformatics approach provides a promising bio compound Anonaine from *A. squamosa* as a possible addition to the natural concoctions that can be used in disease management of rice blast. Addition of *A. Squamosa* leaves during extraction of natural concoctions may give better results in managing the rice blast.

Acknowledgement

The authors acknowledge valuable inputs from Mrs T. Sridevi, Scientific Officer from National Institute of Plant Health Management and Dr. B. R. Ambedkar University, Srikakulam for providing space and lab facilities.

Conflict of interest

The author(s) declare no conflicts of interest concerning this article's research, authorship, and/or publication.

References

1 Pari S and Sarah J G, Against the grain: Safeguarding rice from rice blast disease, *Trends Biotechnol*, 2008, **27**, 141-150, doi: 10.1016/j.tibtech.2008.12.002.

2 Zeigler R S, Leong S A and Teeng P S, Rice blast disease, *Elsevier*, 1994, **51(3)**, 367-369, doi: 10.13140/ RG.2.2.34303.53924.

3 Das S R and Naik B S, Progress of rice research in Odisha (1965-2015) A technical report, *Research gate,* 2015, doi: 10.13140/RG.2.2.10536.98563.

4 Long D H, Lee F N and Tebeest D O, Effect of nitrogen fertilisation on disease progress of rice blast on susceptible and resistant cultivars, *Plant Dis*, 2000, **84**, 403-409, doi: 10.1094/PDIS.2000.84.4.403.

5 Li-Wei L, Sheng-Hsin H, Su-Ju L, Yu-Min W and Wen-Shin L, Rice blast (*Magnaporthe oryzae*) Occurrence prediction and the key factor sensitivity analysis by machine learning, *Agronomy*, 2021, **11**, 771, doi: 10.3390/agronomy11040771.

6 Dean R A, Talbot N J, Ebbole D J, Farman M L, Mitchell T K, *et al.*, The genome sequence of the rice blast fungus *Magnaporthe grisea, Nature*, 2005, **434**, 980-986, doi: 10.1038/nature03449.

7 Hamer J E, Howard R J, Chumley F G and Valent B A, Mechanism for surface attachment in spores of a plant pathogenic fungus, *Science*, 1988, **239**, 288–290, doi: 10.1126/science.239.4837.288.

8 Bourett T M and Howard R J, Actin in penetration pegs of the fungal rice blast pathogen, *Magnaporthe grisea*, *Protoplasma*, 1992, **168**, 20–26, doi: 10.1007 /BF01332647.

9 Prasanna K, Kirk C and Barbara V, Roles for rice membrane dynamics and plasmodesmata during biotrophic invasion by the blast fungus, *Plant Cell*, 2007, **19(2)**, 706-724, doi: 10.1105/tpc.106.046300.

10 De Jong J C, McCormack B J, Smirnoff N and Talbot N J, Glycerol generates turgor in rice blast, *Nature*, 1997, **389**, 244–245, doi: 10.1038/38418.

11 Kurschner E, Bonman J M, Garrity D P, Tamisin M M, Pabale D, *et al.*, Effects of nitrogen timing and split application on blast disease in upland rice, *Plant Disease*, 1992, **76**, 384-389, doi: 10.1094/PD-76-0384.

12 Seebold K W, Kucharek T A, Datnoff L E, Correa-Victoria F J and Marchetti M A, The influence of silicon on components of resistance to blast in susceptible, partially resistant cultivar of rice, *Phytopathology*, 2001, **91**, 63-69, doi: 10.1094/PHYTO.2001.91.1.63.

13 Magar P B, Acharya B and Pandey B, Use of chemicals for the management of rice blast (*Pyriculariagrisea*) disease, *Int J Appl Sci Biotechnol*, 2015 **3**(3), 474-478, doi: 10.3126/ijasbt.v3i3.13287.

14 Vidhyasekaran P, Rabindran R, Muthamilan M, Nayar K, Rajappan K, *et al.*, Development of a powdery formulation of Pseudomonas fluorescence for control of rice blast, *Plant Pathol*, 1997, **46**, 291-297, doi: 10.1046/j.1365-3059.1997.d01-27.x.

15 Rajappar K, Ushamalini C, Narasimhan N, Abdul V and Kareem A, Management of grain discoloration of rice with solvent-free EC formuations of neem and pungam oils, *Phytoparasitica*, 2001, **29**(2), 171-174, doi: 10.1007/BF02983962.

16 McArthur J B and Chen X, Glycosyltransferase engineering for carbohydrate synthesis, *Biochem Soc Trans*, 2016, **44**(1), 129-42, doi: 10.1042/BST20150200.

17 Mio T, Adachi-Shimizu M, Tachibana Y, Tabuchi H, Inoue S B, *et al.*, Cloning of the *Candida albicans* homolog of *Saccharomyces cerevisiae* GSC1/FKS1 and its involvement in beta-1,3-glucan synthesis, *J Bacteriol*, 1997, **179**(13), 4096–4105, doi: 10.1128/jb.179.13.4096-4105.1997.

18 James S K, Aki Y, Morgann C R, Indrani B and Doering T L, Glycosyltransferases and their products: Cryptococcal variations on fungal themes, *FEMS Yeast Res*, 2006, **6**(4), 499–512, doi: 10.1111/j.1567-1364.2006.00054.x.

19 Varki A, Cummings R D and Esko J D, Glycosyltransferases and glycan-processing enzymes, In *Essentials of glycobiology*, 4th edn, (Cold Spring Harbor Laboratory Press), 2009, doi: 10.1101/glycobiology.4e.6.

20 Fernández-Alvarez A, Elías-Villalobos A and Ibeas J I, The O-Mannosyltransferase PMT4 is essential for normal appressorium formation and penetration in ustilago maydis, *Plant Cell*, 2009, **21**(10), 3397–3412, doi: 10.1105/tpc.109.065839.

21 Mikolajczyk K, Kaczmarek R and Czerwinski M, How glycosylation affects glycosylation: The role of N-glycan's in glycosyltransferases activity, *Glycobiology*, 2020, **30**(12), 941-969, doi: 10.1093/glycob/cwaa041.

22 Li H T, Wu H M, Chen H L, Liu C M and Chen C Y, The pharmacological activities of (−)-anonaine, *Molecules*, 2013, **18**(7), 8257–8263, doi: 10.3390/molecules18078257.

23 Richard P Pohanish, *Sittig's Handbook of Pesticides and Agricultural Chemicals*, 2nd Edn, (William Andrew Publishing, USA), 2015.

24 Majeed S, The state of the curcumin market, *Nat Prod Insider*, 2015, **3**(2), 3-6, doi: 10.1021/ acs.jmedchem.6b00975.

25 Andrew W, Martino B, Stefan B, Gabriel S, Gerardo T, *et al.*, SWISS-MODEL: homology modelling of protein structures and complexes, *Nucleic Acids Res*, 2018, **W1**, W296–W303, doi: 10.1093/nar/gky427.

26 Colovos C and Yeates T O, Verification of protein structures: Patterns of non bonded atomic interactions, *Protein Sci*, 1993, **2**(9), 1511-1519, doi: 10.1002/pro.5560020916.

27 Tian W, Chen C, Lei X, Zhao J and Liang J, CASTp 3.0: Computed atlas of surface topography of proteins, *Nucleic Acids Res*, 2018, **46**, 363-367, doi: 10.1093/nar/gky473.

28 Dallakyan S and Olson A J, Small Molecule library screening by Docking with PyRx, *Methods Mol Biol*, 2015, **1263**, 243-250, doi: 10.1007/978-1-4939-2269-7_19.

29 Berendsen H J C, Van der Spoel D and Van Drunen R, GROMACS: A message-passing parallel molecular dynamics implementation, *Comput Phys Commun*, 1995, **91**(1-3), 43-56, doi: 10.1016/0010-4655(95)00042-E.

30 Vanommeslaeghe K, Hatcher E, Acharya C, Kundu S, Zhong S, *et al.*, CHARMM general force field: A force field for Drug-Like molecules compatible with the CHARMM all-atom additive biological force field, *J Comput Chem*, 2010, **31**, 677-690, doi: 10.1002/jcc.21367.

31 Chan K N, Khaing A A, Phyoe A, Thida M, Myo W W, *et al.*, Bio-efficacy of *Annona squamosa*, *Azadirachta indica* and *Artocarpus heterophyllus* against fall armyworm, *Bull Insectology*, 2023, **76**(2) 189-196.

32 Muthu R, Vishnupriya R, Uma D and Santhanakrishnan V P, Insecticidal activity and changes in midgut histology of the generalist herbivore, Spodoptera litura F. (Lepidoptera: Noctuidae) in response to seed extract of *Annona squamosa* Linn, *J Appl Nat Sci*, 2023, **15**(1), 401-407, doi: 10.31018/jans.v15i1.4371.

33 Joshi T, Sharma P, Chandra S and Pande V, Molecular docking and molecular dynamics simulation approach to screen natural compounds for inhibition of *Xanthomonas oryzae pv. Oryzae* by targeting peptide deformylase, *J Biomol Struct Dyn*, 2021, **39**(3), 823-840, doi: 10.1080/07391102.2020.1719200.

34 He F, Wang X, Wu Q, Liu S, Cao Y, *et al.*, Identification of potential ATP-competitive cyclin-dependent kinase 1 inhibitors: De novo drug generation, molecular docking, and molecular dynamics simulation, *Comput Biol Med*, 2023, **155**, 106645, doi: 10.1016/j.compbiomed.2023.106645.

35 Liu Y, Liu Z, Zeng G, Chen M, Jiang Y, *et al.*, Effect of surfactants on the interaction of phenol with laccase:

Molecular docking and molecular dynamics simulation studies, *J Hazardous Mater*, 2018, **357**, 10-18, doi: 10.1016/j.jhazmat.2018.05.042.

36 Sahar H and Jeffrey J C, Targeting the fungal cell wall: Current therapies and implications for development of alternative antifungal agents, *Future Med Chem*, 2019, **11**(8), 869-883, doi: 10.4155/fmc-2018-0465.

37 Deng S, Sun W, Dong L, Cui G and Deng Y Z, *MoGT2* is essential for morphogenesis and pathogenicity of *Magnaporthe oryzae*, *Msphere*, 2019, **4**(10), 309-319, doi: 10.1128/mSphere.00309-19.

38 Ibrahim M A A, Abdeljawaad K A A, Roshdy E, Mohamed D E, Ali T F, *et al.*, *In silico* drug discovery of SIRT2 inhibitors from natural source as anticancer agents, *Sci Rep*, 2023, **13**, 2146, doi: 10.1038/s41598-023-28226-7.

39 Pratibha V D, Hooli A A and Holihosur S N, Bioefficacy of cold ethyl alcohol extract of *Annona squamosa* against *Spodoptera litura Fabricius*, *J Biopesticides*, 2010, **3**, 271–274.